XII International Conference on Computational Plasticity. Fundamentals and Applications
COMPLAS XII
E. Oñate, D.R.J. Owen, D. Peric and B. Suárez (Eds)

NONLOCAL APPROACH FOR THE ANALYSIS OF DAMAGE IN HYBRID MASONRY UNDER CYCLIC LOADING

ILINCA STANCIULESCU*, ZHENJIA GAO* AND MIHAELA NISTOR*

* Rice University
Department of Civil and Environmental Engineering
6100 Main Street, MS 318, Houston, TX 77005, USA
e-mail: ilinca.s@rice.edu

Key words: Continuum Damage Mechanics, Nonlocal Damage Models

Abstract. Hybrid masonry is a recent technology that facilitates the use of concrete masonry unit blocks in connection with steel components in seismic areas. A continuum damage mechanics formulation is utilized due to the quasi-brittle character of masonry panels. A two scalar damage model that accounts for tension and compression is implemented with its local and nonlocal formulation. The nontrivial process of calibrating the parameters is addressed and numerical examples are presented to demonstrate the capabilities of the computational framework utilized.

1 INTRODUCTION

Designing buildings in seismic areas lead to the rise of new technologies. Such a technology for earthquake resistant design of buildings, known as hybrid masonry, has emerged recently. In this system, reinforced masonry walls are designed as stiff, strong and ductile panels, interacting with the surrounding steel frame to resist lateral seismic forces. In the hybrid masonry structural system, the panels are not only used to provide spatial functionality in a building, but also to enhance the seismic performance. Steel frames are attached to masonry panels and transfer part of the loading (e.g., gravity forces, story shears and overturning moments) to the masonry [2].

Based upon the method used to construct the hybrid masonry structural system, the mechanisms to transfer loads from the steel frame to the masonry panel are different. Thus, the hybrid masonry systems are classified into Type I, Type II and Type III hybrid walls. In Type I hybrid wall there is a gap between the steel frame and the masonry panel. The beam is connected to the masonry panel through connector plates, which allow only for the transfer of horizontal forces. The gap surrounding the masonry panel and the steel frame does not allow for the transfer of axial loads and in-plane shear at columns

(Figure 1(a)). Type II and Type III walls are shown in Figure 1(b) and Figure 1(c). The Type II wall has no gap between the beam and the masonry panel, allowing for vertical load transfer from the frame to the masonry panel in addition to the horizontal forces from Type I. The Type III wall has no gaps between the steel frame and the masonry panel and allows for the most load transmission (i.e., horizontal and vertical forces from the beam to the panel, and in-plane shear at column).

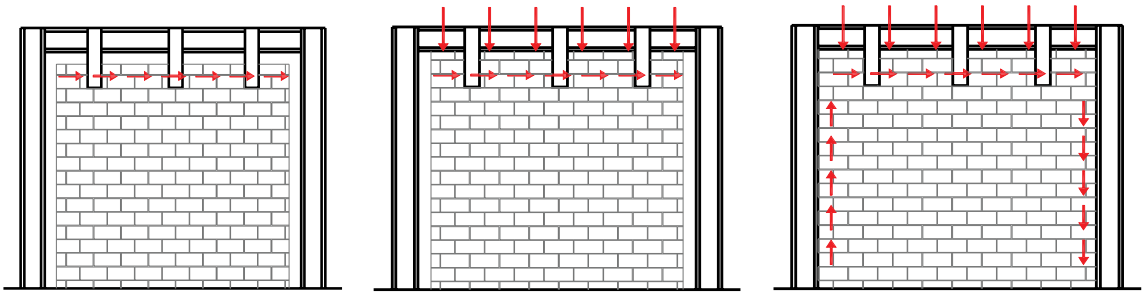

(a) Type I (b) Type II (c) Type III

Figure 1: Hybrid masonry systems

In order to apply this new technology, it is important to have a framework that correctly predicts the propagation of damage in the masonry panel, and has the capability to evaluate the loading capability of the hybrid system. The masonry walls are made of hollow concrete blocks. Quasi-brittle materials, such as concrete, have very high compression strength, but very low resistance in tension. Size effects, tension softening, tension hardening, tension stiffening, bond-slip, concrete confinement, creep and other non-linear effects have a substantial impact on the structural behavior and need to be taken into account in the simulations of such structures.

Several approaches are available to model concrete damage due to tension. One approach is the discrete crack model (DCA), which simulates the propagation of isolated cracks in plain concrete using fracture mechanics concepts [11]. This approach has the disadvantage of requiring re-meshing of the domain as the crack surface changes. Another approach is the smeared crack approach (SCA) that uses a continuum model [5]. Because the SCA exibits severe stress locking, the co-rotational crack model [1] was introduced as an improvement.

In this work a continuum damage mechanics formulation is utilized to capture the propagation and distribution of damage in the masonry panels. This approach models the material degradation due to micro cracking, interfacial de-bonding and other similar defects [3]. These changes in the microstructure lead to a degradation of material stiffness observed on the macro scale. A two scalar damage model [9] that accounts for damage in tension and compression is implemented. Damage models can have local and non-local forms. Local damage models have a straightforward implementation, but suffer from

stress locking (damage is limited to an arbitrarily small volume of material) and lead to numerical results that become pathologically sensitive to the mesh size. A nonlocal damage approach is utilized here to avoid this pathological sensitivity. The idea behind the nonlocal algorithm is that the stress at a point depends on the state of the whole body [4]. When the equivalent strain of point is computed, all points within a radius l_R (characteristic length) around the point will contribute with a certain weight.

The rest of the paper is organized as follows. In section 2 a description of the computational model is presented. Section 3 outlines the procedure for the calibration of the model parameters and some numerical examples are presented in section 4 to demonstrate the capabilities of the computational framework utilized.

2 DESCRIPTION OF COMPUTATIONAL MODEL

The computational model is implemented in FEAP (Finite Element Analysis Program) [12], an open source code that provides a framework for finite element simulations. The formulations for the components of the computational model of the hybrid masonry system are discussed in this section; they are a mix of FEAP original elements and user implemented functions.

The masonry is modeled using a two scalar damage model [9] with a non-local formulation. The constitutive law is written in the form:

$$\boldsymbol{\sigma} = (1-\omega)\boldsymbol{D}\boldsymbol{\varepsilon} \ , \tag{1}$$

where $\boldsymbol{\sigma}$ is the stress, $\boldsymbol{\varepsilon}$ is the engineering strain, $\boldsymbol{D}$ is the elastic material stiffness tensor, and ω is the damage variable. For a totally damaged material $\omega = 1$, while for the undamaged state $\omega = 0$.

The two scalar damage model utilized couples the responses from tension and compression and defines the total damage coefficient ω as the weighted average of the damage coefficients for tension (ω_t) and compression (ω_c):

$$\omega = \alpha_t \omega_t + \alpha_c \omega_c \ , \tag{2}$$

where the weights α_t and α_c are functions of the principal strains:

$$\begin{aligned} \alpha_t &= \sum_{i=1}^{3} \left[\frac{\varepsilon_{ti} < \varepsilon_{ci} + \varepsilon_{ti} >}{\bar{\varepsilon}^2} \right]^{\beta} \\ \alpha_c &= \sum_{i=1}^{3} \left[\frac{\varepsilon_{ci} < \varepsilon_{ci} + \varepsilon_{ti} >}{\bar{\varepsilon}^2} \right]^{\beta} . \end{aligned} \tag{3}$$

ε_{ti} is the positive strain due to positive stress, ε_{ci} is the positive strain due to negative stress, $\bar{\varepsilon}$ is the equivalent strain, and β is a factor that is used to reduce the effect of damage under shear force.

The equivalent strain is defined as:

$$\bar{\varepsilon} = \sqrt{\sum_{I=1}^{3} < \varepsilon_I >^2} \ , \tag{4}$$

where ε_I, I = 1,2,3 are the principal strains, and the brackets $< \cdot >$ denote the positive part of the quantity.

The damage coefficients from equation 2 are evaluated using the functions:

$$\omega_t = \begin{cases} 0 & \text{if } \kappa \leq \varepsilon_0 \\ 1 - \frac{\varepsilon_0(1-A_t)}{\kappa} - \frac{A_t}{e^{B_t(\kappa-\varepsilon_0)}} & \text{if } \varepsilon_0 \leq \kappa \ , \end{cases} \tag{5}$$

$$\omega_c = \begin{cases} 0 & \text{if } \kappa \leq \varepsilon_0 \\ 1 - \frac{\varepsilon_0(1-A_c)}{\kappa} - \frac{A_c}{e^{B_c(\kappa-\varepsilon_0)}} & \text{if } \varepsilon_0 \leq \kappa \ , \end{cases}$$

where κ is the largest equivalent strain obtained in history of loading. The parameters are discussed in Section 3. In an attempt to better capture the behavior of masonry in tension [7], the damage coefficient for tension (ω_t) in equation 5 is evaluated as:

$$\omega_t = \begin{cases} 0 & \text{if } \kappa \leq \varepsilon_0 \\ 1 - \frac{\varepsilon_0}{\kappa} e^{-\frac{\kappa-\varepsilon_0}{\varepsilon_f-\varepsilon_0}} & \text{if } \varepsilon_0 \leq \kappa \leq \varepsilon_f \ . \end{cases} \tag{6}$$

Here, ε_0 and κ have the same meaning as before, while ε_f is a parameter controlling the post-peak slope (the softening branch).

The steel components of the hybrid masonry system (i.e., the steel frame, the reinforcement bars and the connector plates) are modeled using build-in FEAP elements that account for plasticity with hardening.

3 PARAMETER CALIBRATION

The computational model outlined in the previous section requires calibration of parameters before using it for the prediction of the hybrid masonry system behavior under cyclic loading. Calibration of the model parameters for the two scalar damage model is not a trivial process. The model is designed to capture the damage of brittle materials (in a continuum damage approach) in both tension and compression, with model parameters that are designed to provide a homogenized description of what is in reality a process in a composite material.

The nine parameters that need to be calibrated are E (modulus of elasticity for masonry), ε_0 (initial damage threshold), ν (Poisson's ratio), A_t, B_t, A_c, B_c, β, l_R (characteristic length). They interact in complex ways and influence the global response. The versatility of the model is paid by the lack of physical meaning for some of the parameters.

Identification of parameters falls into the class of inverse problems. Ideally, a variety of experimental tests provide the data necessary to calibrate parameters in damage models.

Thus, Young's modulus (E) and Poisson's ratio (ν) can be determined from the elastic part of uniaxial compression data and Brazilian test. Parameters ε_0, A_c, B_c and l_R are calibrated based on the rest of the compression / Brazilian test data ($\varepsilon_0 = \frac{f_t}{E}$, where f_t is the maximum tensile strength). Moreover, a relationship can be determined between A_c, B_c and ε_0, by ensuring that the uxiaxial compressive stress-strain curve has a continuous variation of slope [6]:

$$\begin{aligned} B_c &< \frac{1}{\varepsilon_0} \\ A_c B_c \varepsilon_0 &= A_c - 1 \end{aligned} \tag{7}$$

Parameters A_t, B_t and β are calibrated using data from several different experiments under complex loading. Alternatively, if equation 6 is used for the damage coefficient for tension (ω_t), parameters ε_0 and ε_f are calibrated from the such tests.

In the literature, ranges are provided for some of the parameters, but the calibration procedure remains a nontrivial proccess. After the parameters are calibrated, the model can be successfully applied to predict the behavior of hybrid masonry systems under cyclic loading.

4 NUMERICAL EXAMPLES

This section provides numerical examples that illustrate the capabilities of the computational model. The two scalar damage model is tested against experimental data. The experimental data used in the first numerical example is part of a reasearch project that investigates the influence of the reinforcing steel on the shear strength and ductility of the masonry panel, along with the influence of the reinforcement content and axial compressive strength on the failure mechanisms (for more details see [8]).

A number of sixteen walls were tested [8]. For each of the panel walls in the experiment the aspect ratio was kept constant (height/length ratio equal to 1). The masonry panels were fully grouted, had a reinforced top beam, a base slab and reinforcing steel uniformly distributed in each direction. In-plane axial and lateral load were applied through hydraulic actuators and the masonry panel acted as a cantilever wall with free rotation at the top and the base slab fixed to the strong floor.

We present here results that correspond to wall specimen number 5, which is 6 ft (1.83 m) high, 6 ft (1.83 m) long built of 6" $\times$ 8" $\times$ 16" hollow concrete blocks, with five vertical #7 (22.225 mm) and five horizontal #3 (9.525 mm) reinforcing steel bars spaced at 16 in (40.6 cm). The average compressive stength of masonry units obtained from material tests is 2,400 psi (16.55 MPa) and the average tensile strengths of the reinforcing steel are provided in Table 1. The specimen was subject to standard lateral displacement history, which consisted of sequences of fully reversed displacement cycles (Figure 2(a)), under constant axial load of 40 kips (178 kN).

The finite element model includes the masonry panel, and vertical and horizontal reinforcement. Four node quadrilateral elements with 2×2 Gauss points are used to model

Table 1: Average tensile strengths of reinforcing steel

Bar number	Yield strength (ksi)	Ultimate strength (ksi)
3	56	81
7	72	103

the masonry panel, with a mesh size for the panel chosen such that is equal to the experimentally observed dimension of the compressive fracture zone at the base of wall panels [8]. It is known that this approach alleviates the mesh-size sensitivity issue and therefore the use of nonlocal formulation can be avoided. The parameters of the computational model described in Section 2 are calibrated using the material test data. In this example, the damage coefficient for tension is given by equation 6. A set of parameters identified is: $\varepsilon_0 = 0.00049$, $\varepsilon_f = 0.06$, $Ac = 1.33$, $Bc = 511.3$, $\beta = 1$, the modulus of elasticity for masonry $E = 3.4 \times 10^3 MPa$, $\nu = 0.16$. The parameters are in agreement with the restrictions given in equation 7. The modulus of elasticity and Poisson's ratio used for steel components are $E_s = 2 \times 10^{11} MPa$ and $\nu = 0.26$.

The load-displacement hysteresis curve obtained in FEAP is shown in Figure 2(b). The horizontal load represents the total horizontal reaction at the base of the masonry wall and the displacement corresponds to the top points of the wall, where displacement control is applied (Figure 2(a)). The numerical results match well the experimental data and demonstrate that the framework introduced can capture the masonry behavior under cyclic loading.

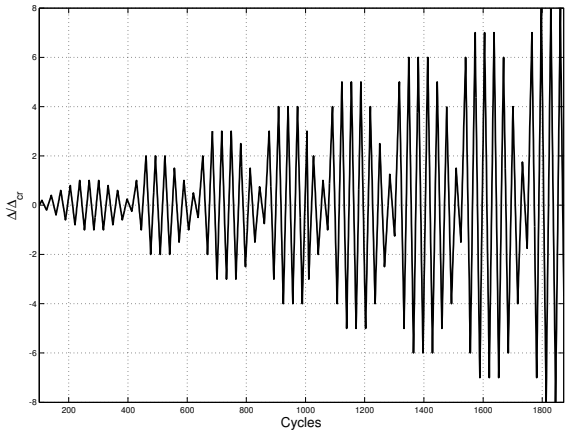

(a) Displacement history

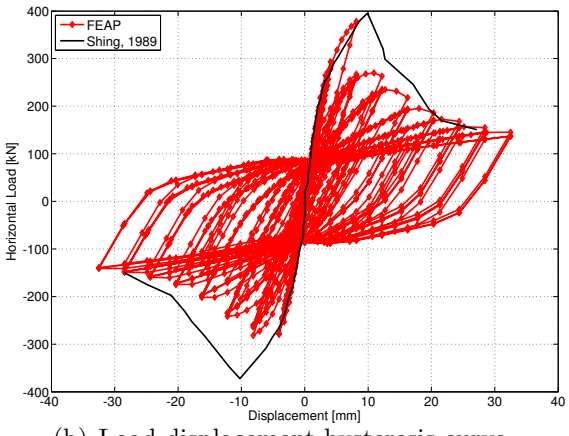

(b) Load-displacement hysteresis curve

Figure 2: Cyclic loading and load-displacement hysteresis curve

The second numerical example uses experimental data from the third phase of an ongoing research project conducted at University of Hawaii at Manoa (UHM). The project

investigates the applicability of the hybrid masonry system in seismic areas. Several wall specimens have been constructed, but the experimental data used in this example corresponds to the fully grouted case (for more details see [10]).

The hybrid masonry system analyzed is composed of a masonry panel, a steel frame and connector plates. The masonry panel uses standard 8" × 8" × 16" concrete masonry unit blocks and is 6'-8" long (2.03 m), 2'-8" high (0.81 m), corresponding to the length of five blocks and the height of four courses. The masonry panel lies on a 6' concrete slab that is cast above a $W24 \times 76$ steel beam. The steel beam is securely anchoring the wall specimen to the strong floor of the laboratory during testing. The reinforcement in the masonry panel consists of four vertical and one horizontal #5 (16 mm) bars, with two of the vertical reinforcement bars placed centrally in the two end cells and the other two vertical reinforcement bars at 24" (0.61 m) from them. The horizontal reinforcement is placed in the second course from the top. A $W18 \times 40$ steel beam is supported 1" above the masonry panel by two pin-ended vertical load rods. The beam transfers the horizontal load from the hydraulic actuator through the connector plates to the masonry panel. Two pairs of connector plates are secured with through-bolts on each side of the wall.

The materials test data provided the steel properties for the connector plates and for the reinforcing steel bars (Table 2). An example of the experimental fit for connectors is shown in Figure 3.

Table 2: Average tensile strengths for connector plates and reinforcing steel bars

Specimen	Yield strength (ksi)	Ultimate strength (ksi)	Young's Modulus (ksi)
Connector	50	80	30000
#5	68	100	30000

The finite element model accounts for the steel frame, the masonry panel, the reinforcement within the panel and the connector plates. The frame is pinned at the base of the columns, the masonry is fixed at base and the connectors are fixed at the upper part to the frame and tied horizontally at the lower part to the masonry. This example uses a nonlocal formulation and the damage coefficient for tension from equation 5. The parameters calibrated from the material tests are: $\varepsilon_0 = 0.0001$, modulus of elasticity for masonry $E = 4.6 \times 10^2\ MPa$, $\nu = 0.2$, $A_t = 0.3$, $B_t = 10$, $A_c = 1.02$, $B_c = 200$, $\beta = 1.35$ and $l_R = 0.025\ m$. They comply with the specifications in equation 7.

The force-displacement hysteresis curve obtained from the FEAP simulation and the envelope of the experimental data are shown in Figure 4. The force stands for the total horizontal reaction at the base of the wall and the displacement is the applied displacement at the top through the steel beam. The FEAP results match the experimental data, confirming the capabilities of the utilized framework.

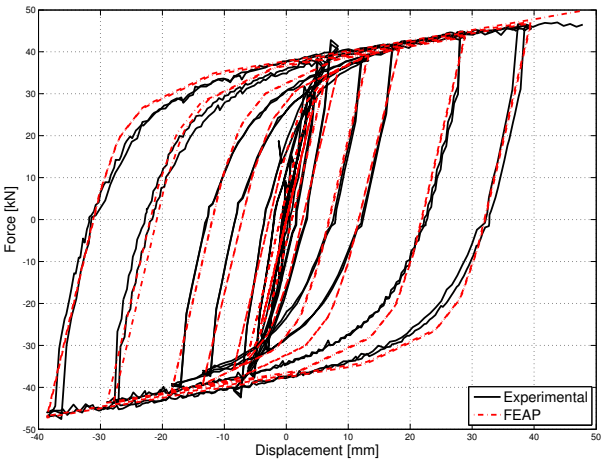

Figure 3: Masonry reaction vs. displacement of top of connector

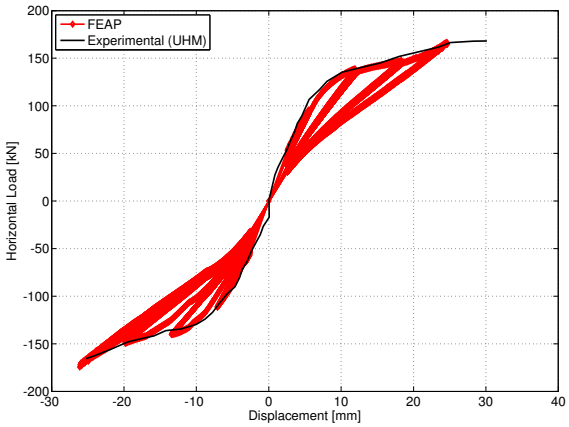

Figure 4: Load-displacement hysteresis curve

5 CONCLUSIONS

Hybrid masonry systems are modeled through a continuum damage mechanics approach. The calibration of parameters is not a trivial process but the versatility of the two scalar damage model is demonstrated and supports its use for modeling the propagation of damage in the hybrid systems. Two numerical examples are provided and the analysis results are compared to experimental data. The numerical examples demonstrate the capabilities of the framework to capture the behavior of hybrid masonry under cyclic loading.

ACKNOWLEDGEMENTS

The work has been funded in part by NSF under the grant no. CMMI 0936464. This support is greatly appreciated.

Experimental data was provided by professor Ian Robertson (University of Hawaii at

Manoa) and professor Dan Abrams (University of Illinois at Urbana-Champain).

Support was also received from the Data Analysis and Visualization Cyberinfrastructure funded by NSF under grant OCI-0959097.

REFERENCES

[1] Z P Bazant. Comment on orthotropic models for concrete and geomaterials. *Journal of Engineering Mechanics*, 109(3):849–865, 1983.

[2] D T Biggs. Hybrid Masonry Structures. *Proceedings of the Tenth North American Masonry Conference, The Masonry Society, Boulder, CO*, 2007.

[3] Y Calayir and M Karaton. A continuum damage concrete model for earthquake analysis of concrete gravity dam-reservoir systems. *Soil Dynamics and Earthquake Engineering*, 25(11):857–869, 2005.

[4] P. Duhem. Le potentiel thermodynamique et la pression hydrostatique. *Ann. Ecole Norm*, 10:187–230, 1893.

[5] R Espandar and V Lotfi. Comparison of non-orthogonal smeared crack and plasticity models for dynamic analysis of concrete arch dams. *Computers and Structures*, 81(14):1461–1474, 2003.

[6] Guenter Hofstetter and Guenther Meschke, editors. *Numerical Modeling of Concrete Cracking*. Springer, 2011 edition, September 2011.

[7] M Jirásek. Non-local damage mechanics with application to concrete. *Revue Française de Génie Civil*, 8:683–707, 2004.

[8] H R Lotfi and P.B. Shing. An appraisal of smeared crack models for masonry shear wall analysis. *Computers and Structures*, 41(3):413–425, 1991.

[9] J Mazars. Description of the Behaviour of Composite Concretes Under Complex Loadings Through Continuum Damage Mechanics. In *Proceedings of the U.S. National Congress of Applied Mechanics*, pages 135–139, 1986.

[10] Steven Mitsuyuki. Verification of Fuse Connector Performance for Hybrid Masonry Seismic Structural Systems. Master's thesis, University of Hawaii at Manoa, April 2012.

[11] Petter E Skrikerud and Hugo Bachmann. Discrete Crack Modelling for Dynamically Loaded, Unreinforced Concrete Structures. *Earthquake Engineering and Structural Dynamics*, 14(2):297–315, 1986.

[12] R.L. Taylor and University of California, Berkeley. Dept. of Civil and Environmental Engineering. FEAP, a Finite Element Analysis Program: Version 8.3 User Manual. 2011.